Journal of Applied Remote Sensing

RemoteSensing.SPIEDigitalLibrary.org

Continuous monitoring of biophysical *Eucalyptus* sp. parameters using interferometric synthetic aperture radar data in P and X bands

Fábio Furlan Gama
João Roberto dos Santos
José Claudio Mura

SPIE.

Fábio Furlan Gama, João Roberto dos Santos, José Claudio Mura, "Continuous monitoring of biophysical *Eucalyptus* sp. parameters using interferometric synthetic aperture radar data in P and X bands," *J. Appl. Remote Sens.* **10**(2), 026002 (2016), doi: 10.1117/1.JRS.10.026002.

Continuous monitoring of biophysical *Eucalyptus* sp. parameters using interferometric synthetic aperture radar data in P and X bands

Fábio Furlan Gama,* João Roberto dos Santos, and José Claudio Mura
National Institute for Space Research-INPE, Av. dos Astronautas, 1758, P.O. BOX 515, São José dos Campos, SP, São Paulo CEP 12227-010, Brazil

Abstract. This work aims to verify the applicability of models obtained using interferometric synthetic aperture radar (SAR) data for estimation of biophysical *Eucalyptus saligna* parameters [diameter of breast height (DBH), total height and volume], as a method of continuous forest inventory. In order to obtain different digital elevation models, and the interferometric height (Hint) to retrieve the tree heights, SAR surveying was carried out by an airborne interferometric SAR in two frequencies X and P bands. The study area, located in the Brazilian southeast region (S 22°53′22″/W 45°26′16″ and S 22°53′22″/W 45°26′16″), comprises 128.64 hectares of *Eucalyptus saligna* stands. The methodological procedures encompassed: forest inventory, topographic surveying, radar mapping, radar processing, and multivariable regression techniques to build *Eucalyptus* volume, DBH, and height models. The statistical regression pointed out Hint and interferometric coherence as the most important variables for the total height and DBH estimation; for the volume model, however, only the Hint variable was selected. The performance of the biophysical models from the second campaign, two years later (2006), were consistent and its results are very promising for updating annual inventories needed for managing *Eucalyptus* plantations. [DOI: 10.1117/1.JRS.10.026002]

Keywords: remote sensing; synthetic aperture radar; interferometry; Eucalyptus stands; forest inventory; biophysical modeling.

Paper 16013 received Jan. 6, 2016; accepted for publication Mar. 15, 2016; published online Apr. 7, 2016.

1 Introduction

Conventional forest inventory is a time consuming job which must be performed at least once a year for commercial *Eucalyptus* plantations, whose results are usually an extrapolation of the tree structural measurements of some small transects.

Remote sensing techniques make the forest inventory process efficient at inferring tree biophysical parameters, which also allows a synoptic view of the area under analysis. Among the various remote sensing techniques, the use of microwave sensors synthetic aperture radar (SAR) has developed very rapidly in recent years, especially using polarimetry and/or interferometry to study the relationships of biomass and volumetric content of tropical forests in Brazil (Santos et al..;[1] Neeff et al.;[2] Sexton et al.[3]).

Gama et al.[4] used the interferometric airborne SAR data in 2004, from Orbisat Company, operating in X and P bands to obtain models to estimate biophysical parameters (biomass and volume) of homogeneous *Eucalyptus* stands.

Bispo et al.[5] generated a predictive model for biomass estimation in a forested area of Central Amazonia based on the integration of incoherent target scattering decomposition polarimetric attributes, extracted from ALOS-PALSAR data, and geomorphometric variables derived from shuttle radar topography mission, thus improving biomass estimation.

*Address all correspondence to: Fábio Furlan Gama, E-mail: fabio@dpi.inpe.br

Joshi et al.[6] attempted to quantify the effect of forest structure (density, height, and cover fraction) variables by relating ALOS-PALSAR HV backscattering and LIDAR data over broadleaf and conifer stands (planted and natural regeneration forests) to map aboveground biomass (AGB). Santoro et al.[7] looked into the multitemporal datasets from ALOS/PALSAR to assess stem volume retrieval of the boreal forests (Norway spruce, Scotch pine, and deciduous tree species, e.g., birch).

Based on Gama et al.[4] methodology used in 2004, and with data from an interferometric survey carried out in 2006, in X and P bands, with the same radar (Orbisar-1), test site, and flight configuration, it was possible to assess the capacity of the biophysical models generated in 2004 to infer the changes in biophysical parameters in 2006.

The aim of this paper is to verify the applicability of models generated by interferometric SAR data for estimation of biophysical parameters of the *Eucalyptus saligna* stands [diameter at breast height (DBH), height, and volume], as a suitable method for continuous forest inventory.

2 Background

Many approaches have been used to estimate biophysical forest parameters, using SAR data in P and L bands in different polarizations, as well as comparing the correlation between backscatter and biophysical parameters of a pine forest, the results of which pointed out that the estimation of the biomass of branches, trunks, needles, and total biomass was better explained with P-band backscatter than with L-band.

Studies developed by Rauste et al.,[8] in *Pinus* forest, using different frequencies verified that cross-polarized P-band obtained the best correlation between backscatter and forest volume if compared to those of L- and C-bands. A radiometric saturation in C-band of areas with 50 t/ha biomass, and 70 t/ha for L band was also observed.

Pope et al.,[9] using polarimetric SAR data, created some indexes, which showed some relationship with special forest parameters, such as biomass index (BMI), volume scattering index (VSI), canopy scattering index (CSI), and interaction index (ITI).

Borgeaud and Wegmuller,[10] using the interferometric coherence (Coh) obtained by ERS-1 and ERS-2 (C-band), observed that it could help target discrimination. They noticed that deciduous and coniferous forests show the same backscatter intensity, but different coherences, due to the fact that winter season causes leaf loss of deciduous forest, increasing the coherence in C-band.

Kasischke et al.[11] pointed out the occurrence of five types of backscattering mechanisms in vegetation areas: the response from the top of the canopy, from inside the canopy (volume backscatter), from soil through the canopy gaps, from the interaction of soil and trunk, and from shading effects. According to this study, such effects vary with radar wavelength, target surface roughness, soil moisture, vegetation structure and its orientation.

Cloude and Pottier,[12] based on Pauli decomposition and on covariance coherence matrices, could obtain entropy, anisotropy, and alpha angle in order to describe all scattering mechanisms, as the sum of all independent scattering elements thus enabling them to describe the scattering behavior by different regions of the graph of entropy versus alpha angle, where the interactions of dihedral and surface type could be identified.

Le Toan and Floury[13] and Santos et al.[1] observed in their studies a saturation volume of 250 m^3 for P-band in tropical and pine forests. Using SIR-B mission data, Leckie and Ranson[14] observed that P-band beam had a lower attenuation due to coniferous forest components, when compared with C- and L-bands' behavior. According to the authors, as P-band beam had a great penetration in the forest, the correlation coefficient in relation to the trunk was higher if compared with the other spectral bands.

Mura et al.[15] combined P-band coherence, interferometric height (Hint) (digital surface model minus digital terrain model), and X-band image in an IHS image (intensity, hue, and saturation), and used it in a rainforest area in Para State/Brazil, during the AeroSensing Radarsysteme Company surveying. This product allowed distinguishing between primary and secondary forests, increasing the classification rate confidence.

Santos et al.[1] using the AES-1 P-band data from AeroSensing Company in the Tapajos National Forest, Pará state, Brazil, were able to estimate the aerial biomass for the primary

and secondary forest. Based on the statistical analysis, a third-order biomass regression model was carried out from field inventory data and from polarimetric radiometric response. P-band amplitude response in HH and HV polarizations showed a higher correlation with biomass, with a higher determination coefficient ($r^2 = 0.77$) than that of VV polarization ($r^2 = 0.59$).

Neeff et al.[2] and Gama et al.,[4] used interferometric data survey in X- and P-bands, and radiometric response in HH polarization to estimate the biomass of tropical and *Eucalyptus* forests, respectively. An important advantage of using SAR interferometry is that the biomass estimation showed a better result than that of radiometry because it did not show the saturation effect and therefore the prediction models were highly accurate.

Treuhaft et al.[16] reported the sensitivity of X-band interferometric synthetic aperture radar (INSAR) data from the first dual-spacecraft radar interferometer, TanDEM-X, to variations in tropical-forest AGB.

3 Area Under Study

The study area is located in Pindamonhangaba district, São Paulo State, Brazil, at the geographic coordinates 22°53′22″S 45°26′16″W and 22°55′50″S 45°23′06″W. This area is formed by *Eucalyptus saligna* stands, comprising 129 hectares, with tree plantations spaced 3×2 m, located in flat plateaus. The two SAR surveying campaigns were carried out during dry periods, so soil moisture was not considered in this work. Figure 1 shows the study area and the two flight directions in two dates for the airborne SAR data acquisition, the transect positions in red dots, and the corner reflector positions illustrated in yellow triangles.

4 Methodology

Aiming at building regression models to estimate the biophysical variables, we performed several tasks such as microwave data acquisition, topographic survey information, forest dendrometric parameters, and statistical analysis in order to find out the relations between structural metrics and airborne radar response.

The first step of the work in the first campaign was field reconnaissance (December, 2004), to locate the best areas to install the corner reflectors that were used for phase calibration during the interferometric processing for X- and P-bands, as well as for radiometric calibration to obtain the σ^o of P-band images. Each corner reflector was installed on a ground control point (GCP) which had been previously measured by a geodetic differential global positioning system (DGPS).

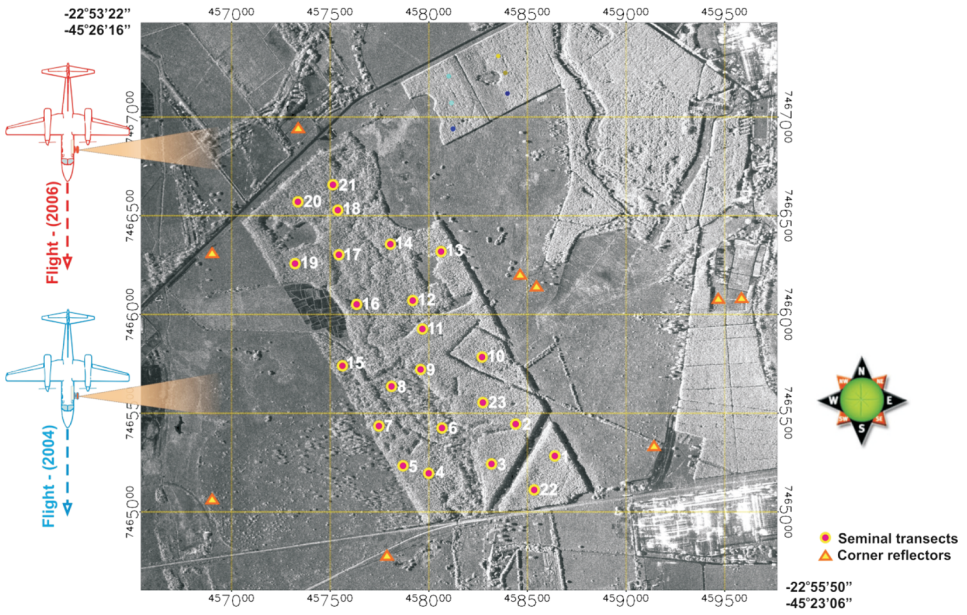

Fig. 1 X-band image of the test site and the inventory plot positions.

These DGPS trackings were carried out by the static relative method, using an official first order satellite base, which allowed obtaining a 5.0-cm plani-altimetric coordinate precision.

In addition to setting up the GCPs, it was necessary to use a high-precision geographic reference point at the same airport used by the airplane. This point was tracked by a geodetic GPS during the flight survey to allow the generation of the attitude vector radar by the airborne inertial measurement unit (IMU) processing.

A topographic survey was carried out using a Topcon total station, model GTS-701, with 3″ of accuracy and 10-m spacing, covering all transects and some pasture areas in order to locate the plots in the images and to evaluate the digital elevation models (DEMs). The measured starting point was the same as the one used to support the corner reflector and to perform the final measurement, which allowed topographic adjustments describing a closed polygon, and which obtained a 5-cm precision in the final adjustments.

For the acquisition of radar data, the OrbiSAR-1 radar from BRADAR Company (Orbisat) was used, which allowed us to generate DEM by SAR interferometry at two different frequencies, X ($\lambda = 3$ cm) and P ($\lambda = 72$ cm) bands.

OrbiSAR-1 operates in four polarizations in P-band, so it was possible to obtain the DEM and the Coh in four different polarizations ($CohP_{HH}$, $CohP_{HV}$, $CohP_{VH}$, and $CohP_{VV}$). Both surveying campaigns (2004 and 2006) obtained final mappings in scale 1: 25,000 for P-band and 1: 10,000 for X-band, whose end pixel size was 2.0 m for P-band and 1.0 m for X-band, with the same values for the respective altimetry. The X-band interferometry was performed in one-pass acquisition with 2.77 m of baseline, generating coherence image, DEM and complex image in HH polarization; while for P-band interferometry, 50 m of baseline was used in two-passes. The difference of the DEM by interferometry in X- and P-bands was considered as Hint, and used as a variable during the building of the regression models.

The biophysical models were built by statistics regression from the SAR surveying and forest inventory in 2004 (Gama et al.[4]), in which the parameters DBH, height, and volume could be estimated from interferometric radar data (σ^o, DEM, and Coh).

In December 2006, a new forest inventory was carried out in the same area and simultaneously a new radar survey was performed with the OrbiSAR-1 airborne radar at the same altitude, speed, incidence angle, and resolution as those of the 2004 radar products, as shown in Fig. 1. Similarly to the 2004 mapping, the corner reflectors for interferometric calibration were set up in the same position. Using the previous biophysical model obtained in 2004, the interferometric products from the 2006 survey were applied and the biophysical estimations were compared with the new forest inventory (2006), as shown on the diagram of Fig. 2.

4.1 *Forest Inventory*

During the radar surveying campaigns in 2004 and 2006, forest inventories were conducted simultaneously in order to characterize the dendrometric parameters according to the annual

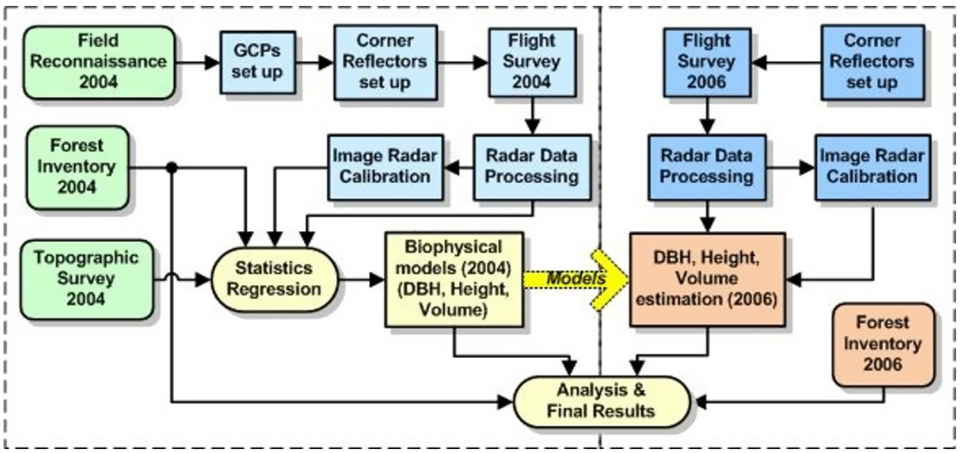

Fig. 2 Methodological procedure.

inventory tracking. The inventory was carried out in 23 independent plots of ~400 m^2 each, in which the DBH and total tree height were measured. Allometric equations based on height, diameter, and form factor were used to calculate tree volume. Equation (1) shows the allometric equation for volume estimation and the corresponding form factors used for each range of DBH measured in the inventory.

$$\text{Volume} = \left(\frac{\text{DBH}^2 * \pi}{4}\right) * \text{TotalHeight} * \text{FF} \qquad \text{FF} = \text{Formfactor} \tag{1}$$

DBH	FF
4.0 – 12.0	0.46
12.0 – 20.0	0.44
20.0 – 28.0	0.42

4.2 *Radar Data Processing*

The Orbisat Company provided the software to process the SAR raw data in order to obtain the images and the interferometry SAR products. The images were processed with four looks to minimize the speckle noise, and then converted to ground range and orthorectified using the corresponding DEM generated during the interferometric processing. Rombach et al.[17] described the details of the data transcription, IMU processing, and SAR data processing to obtain SAR products.

The radiometry of P-band complex images was calibrated by the Radar Tools software (RAT 0.16.2 version), which provided cross talk processing, channel imbalance processing, and polarimetric calibration using a corner reflector response based on Quegan[18] approach.

To calibrate the SAR data, nine corner reflectors of the same size, 1.5-m side length, were distributed between near and far ranges in the area and used for the polarimetric and interferometric calibrations. To acquire σ^o images, the corner reflector peak response was used (Zink et al.,[19] Santos et al.[1]) obtaining a correction factor to transform the P band amplitude images by interactive data language (IDL) routines.

The azimuth and elevation angles of the corner reflectors were calculated based on the flight plan and on the high-accuracy (5 cm) GCP geographic coordinates, the incidence angle of which did not present large variations.

The SAR data was generated using the Orbisat Company software, which allowed obtaining orthorectified SAR images using the corresponding digital elevation models. Details about the Orbisat software for data transcription, IMU and SAR data processing to obtain DEM, orthoimages, and coherences are described by Rombach et al.[17]

The radar cross section of each corner reflector was measured and a linearity behavior was verified. The signal to noise ratio, the antenna pattern, radar losses, and radar illumination geometry were also considered.

The corner reflector responses were also used for the phase calibration during the interferometric calibration in order to obtain the DEM in X and P bands. For polarimetric calibration, the Quegan[18] methodology was used for the cross-talk processing and channel imbalance by these corner reflector responses.

4.3 *Statistical Modeling*

To build the regression models, the variable selection criteria suggested by Neter et al.[20] were used, such as coefficient of determination (r^2), adjusted coefficient of determination (r^2a), Cp criterion (Neter et al.[20]), and Stepwise criterion, using Statistica 6.0 version software.

The coefficient r^2a employs a weighting for the extent of regression adjustment, making it more relevant than the coefficient r^2. Cp criterion involves the concept of total mean square error for each subset of the adjusted regression models, which considers the total error in each value set. Cp criterion can identify subsets of dependent variables in which the total mean squared error is small, i.e., when the Cp value is equal or close to the number of p parameters, this model will be less biased. The forward stepwise procedure gradually adds a new variable to the model, and extracts that part whose contribution was not considered significant by an F-test. Equation (2) shows the Cp criterion estimation

$$\mathrm{Cp} = \left(\frac{\mathrm{SSEp}}{\mathrm{MSE}(X_1, \ldots\ldots X_{p-1})}\right) - (n - 2p), \tag{2}$$

where SSEp is the error sum of squares for the fitted subset regression model with p parameters (with $p - 1 \times$ variables), and mean squared error (MSE).

Levene's test was used for the heteroscedasticity evaluation (constancy of residue variance), which performs the comparison t-test of two subgroups of data set samples to determine whether the average absolute deviation of a subgroup differs from the other. Cook's distance method was used to assess the existence of outliers in the data set (Neter et al.[20]), which considers the influence of a specific observation in all other adjusted values. A sample can be considered an outlier when its percentile of F distribution exceeds 20%.

For model validation of small data sets, prediction sum of squares (PRESS) criterion is used as a way to evaluate the prediction model. The test works by eliminating the i'th case of the data set, estimating the regression function with the remaining observations, then using the adjusted regression equation to obtain the predicted value. The quadratic sum of all these n prediction errors defines the PRESS value. According Neter et al.,[20] the closeness between PRESS and error sum of squares (SSE) values, indicates that the MSE value can be a reasonable indicator of the model predictive ability.

5 Results and Discussion

5.1 *Forest Inventory*

Although the whole plantation area was established in 2000, the average total height of each transect varied widely in its values after having grown for 4 and 6 years, due to the fact that it was a seminal reforestation and the supply of water and nutrients were different inside the site index, compromising the development of the *Eucalyptus* trees. Due to this fact, the occurrence of gaps in the plantation was between 2% and 60% for the plots, in which dead or broken trees were not considered by this criterion. The graph in Fig. 3 shows the total height behavior and its standard deviation for 2004 and 2006 of each plot inventoried.

The mean DBH values of trees inventoried in 2004 and 2006 are shown in Fig. 4, where the newest inventory showed higher values if compared with those of the previous inventory. The floating values happened due to the influence of the kind of plantation (seminal) as well as to the edaphic problems described previously.

The volume values of trees estimated by the allometric equation [Eq. (1)] using the inventory data of 2004 and 2006 are shown in Fig. 5. It can be observed that the latest inventory showed higher values than those of the previous one, as well as a higher standard deviation.

5.2 *Biophysical Models Based on Interferometric Synthetic Aperture Radar 2004 Data Acquisition*

Based on the field data of the first campaign (2004), the regression models for total height and DBH, using criteria r^2, r^2a, Cp and Stepwise, only two variables were selected (LogHint and

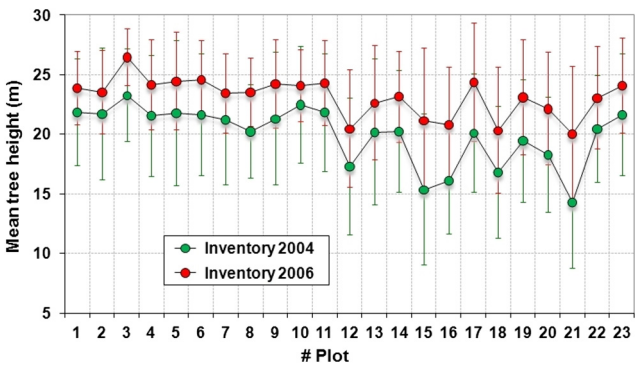

Fig. 3 Height values of *Eucalyptus* stands.

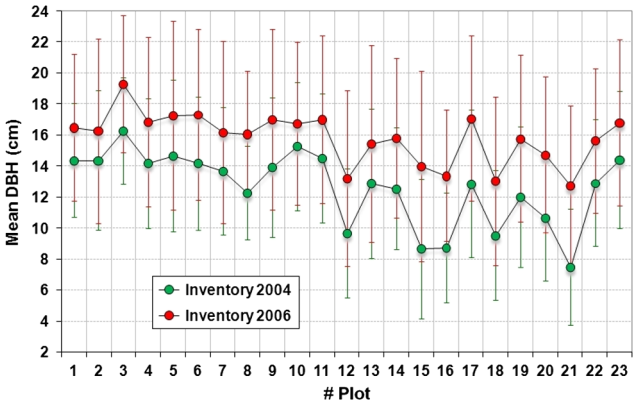

Fig. 4 DBH values of *Eucalyptus* stands.

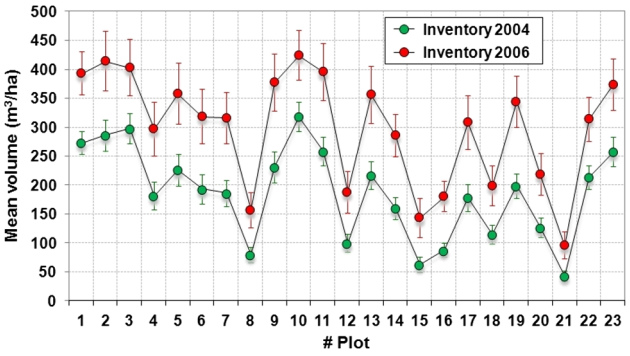

Fig. 5 Volume values of *Eucalyptus* stands.

$CohP_{vv}$), while for the vegetation volume model, only one variable was selected (LogHint) (Table 1).

The DBH model validation by PRESS criterion showed a value which amounted to 25.09, 45.19% being higher than the SSE (17.28), therefore, the MSE value could be used, with a final prediction error of 0.95 cm. This prediction error corresponded to 7.56% compared with the DBH average trees (12.62 cm) and 3.73% compared with the DBH maximum of 25.60 cm.

The total height model validation by PRESS, whose value amounted to 26.78, 49.78% higher than the SSE (17.88), allowed using MSE value to obtain the final prediction error of 0.995 m. Comparing the prediction error with the average tree height (18.75 m) this value corresponded to 5.31%, and if compared with the maximum tree height (23.31 m) this value corresponded to 4.28%.

The forest volume model validation by PRESS criterion (26840.1) was 19.12% higher than the SSE (22532.7), so MSE value was used for obtaining the prediction error of 33.56 m^3. The prediction error compared to the average tree volume (186.33 m^3) corresponded to 18.01%, while for the maximum volume of 318.13 m^3, it corresponded to 10.55%. Table 1 shows the obtained regression models and their determination coefficient.

Table 1 Regression models for bitemporal INSAR acquisition.

Variables	Regression model	r^2	r^2a
DBH	$1.47 + 16.61 \times \text{LogHint} - 13.69 \times \text{CohPvv}$	0.86	0.84
Total height	$7.05 + 17.01 \times \text{LogHint} - 11.74 \times \text{CohPvv}$	0.86	0.84
Volume*	$-314.03 + 427.95 \text{ Log } H_{int}$	0.83	0.83

*Gama et al.[4]

Cook's distance test verified the existence of two outlier cases for total height model and one case for DBH model, while for volume model, four cases were identified. The residues of the regression models presented a tendency to normality by the tests used, having a homoscedasticity behavior according to Levene test. The prediction errors of these models are shown in Table 2. They were estimated based on MSE values obtained for each regression model.

Comparing the DBH regression behavior against forest inventory measures (Fig. 6), there is, on average, a good agreement with the inventoried data, not exceeding the values of the standard deviation of the field inventory, as well as a 3.73% of prediction error. Plot 4 was detected as an outlier (Table 2), and not used in the regression model.

The Hint showed a high variance, with very different values from the total inventory average height value exceeding in many cases, the standard deviation of the measurements, which indicates that the variable Hint alone does not satisfactorily represent the total height of the studied vegetation, as shown in the graph of Fig. 7.

Comparing the total height estimation of each plot with its corresponding inventoried data, it can be noticed that the values were similar, not exceeding the standard deviation values with a 4.28% prediction error (Fig. 8). The two outliers (plots 4 and 8) detected during the regression (Table 2), were not used in the final model.

The volume regression model which uses the LogHint matched the inventory data in some plots; however, in 8 cases their values were different from the inventoried data, exceeding the standard deviation values. Figure 8 graph shows this behavior.

The test site is composed of two plateaus with a flat relief surrounded by a clear pasture, and although plot 8 has a flat relief, its altitude is lower than that of the others, getting flooded part of the year which harms the seedling development phase and damages the development of the trees. Due to this fact, a greater variation of height and canopy size occurred, disturbing the discrimination of ground clearance by DEM in X band. It was also observed that in plot 4, despite some flaws, the height of the trees remained more uniform than that of portion 8.

The standard deviation range of the volume model with a 30 and 40 m^3/ha range; corresponded to an estimation error in the range of 16.1% to 21.47% when compared with the average of the tree volume (186.33 m^3/ha). However, when comparing this standard deviation range

Table 2. Regression models results.

Model	Outliers	PRESS	SSE	MSE	Prediction error	Prediction error
DBH	Plot 4	25.09	17.28	0.909	0.95 cm	3.73%
Total height	Plot 4 and 8	26.78	17.88	0.99	0.99 m	4.28%
Volume	Plot 4, 6, 9, and 19	26840.10	22532.70	1126.60	33.56 m^3/ha	10.55%

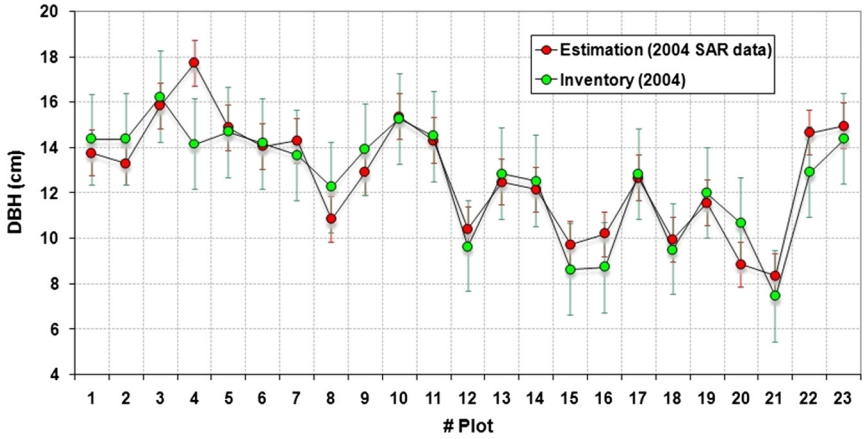

Fig. 6 DBH model and inventory data.

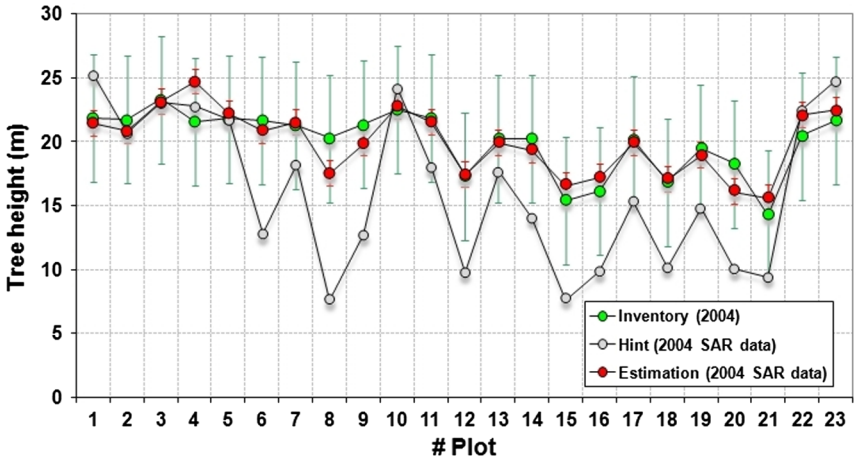

Fig. 7 Total height estimated and inventory data.

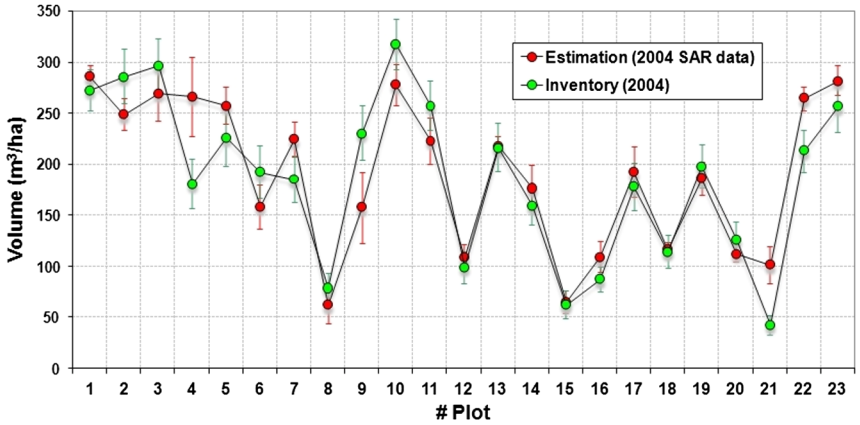

Fig. 8 Volume estimated and inventory data.

with the volume of the biggest trees (318.13 m^3/ha), the error corresponded to a range of 9.43% to 12.57%.

5.3 *Models Performance with Interferometric Synthetic Aperture Radar 2006 Data*

Using the regression model generated in 2004, the DBH estimation for 2006 showed agreement with the inventoried data in relation to the mean values for a great number of cases except 4, which showed an overestimation that surpassed the inventory standard deviation. The graph in Fig. 9 shows the obtained results.

Similar to the DBH estimation, the tree height estimation showed four cases with an overestimation that surpassed the inventory standard deviation. The remaining 19 cases were similar to the inventory or were inside the inventory standard deviation values. The graph in Fig. 10 shows the obtained results.

Analyzing the behavior of the *Eucalyptus* mean height of each plot with its corresponding DBH, a linear relationship between these biophysical variables was observed without significant outliers, whose linear regression showed an r^2 of 0.987 for the 2004 inventory and 0.997 for the 2006 inventory. A progression of height and DBH responses can also be observed, indicating that the vegetative growth at the study area elapsed 2 years. The estimation values of the mean tree heights and the mean DBH, also showed a linear behavior (Fig. 11), like the inventory data, with a continuity of the tendency of the regressions; the 2004 r^2 estimation was 0.991 while it was 0.995 for 2006.

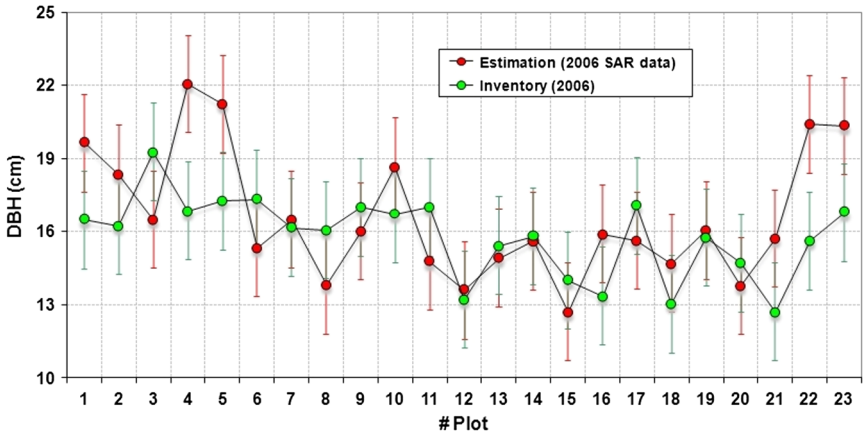

Fig. 9 Mean values of DBH estimation and inventory data.

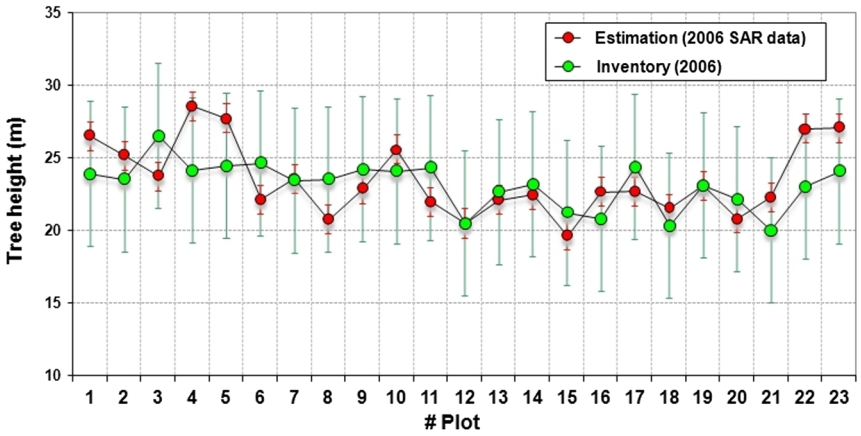

Fig. 10 Mean values of tree height estimation and the inventory data.

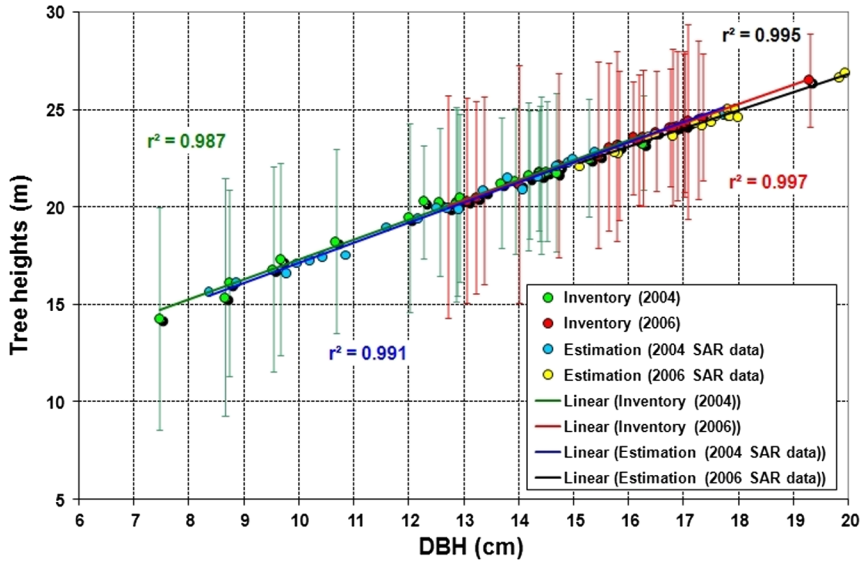

Fig. 11 Mean values of tree height and DBH of *Eucalyptus* stands.

On the other hand, when comparing the inventoried and estimated volume for these two dates, the result was linear with little dispersion, i.e., 0.948 of r^2, while 0.968 for inventoried volume.

Analyzing the tree volume model response, it can be noticed that inventoried and estimated values (Fig. 12) had a linear behavior with a high r^2 value, but an error estimation of 10.55%, acceptable for forest surveying, which considers 10% as a typical inventory error.

Based on the obtained regression models, a hypsometric image for the total height, DBH and volume was generated using the $CohP_{vv}$ and LogHint images, achieving a final image whose pixel values corresponded to numerical values of the regression. For the visualization of a combination of results of the regression model image data and the radiometric response in the X band was performed using the IHS technique (I = intensity, H = hue, S = saturation), which, for all models, was defined: 50% for saturation (S) and the X-band amplitude image as the intensity (I).

The result of the IHS image referring to total height estimation using the SAR from 2004 is shown in Fig. 13(a), along with a range of colors that corresponds to the total height estimated. Color gradients with predominance on the heights of ~14 and ~20 m are shown. The regions of image in blue color correspond to zero point, resulting from settlement failures.

The hypsometric image of Fig. 13(b) corresponds to the total height estimated using the regression model generated in 2004 with the 2006 SAR data. Analyzing the linear regression of the 2006 inventory data and the total height model results, MSE value of 1.39 m was obtained,

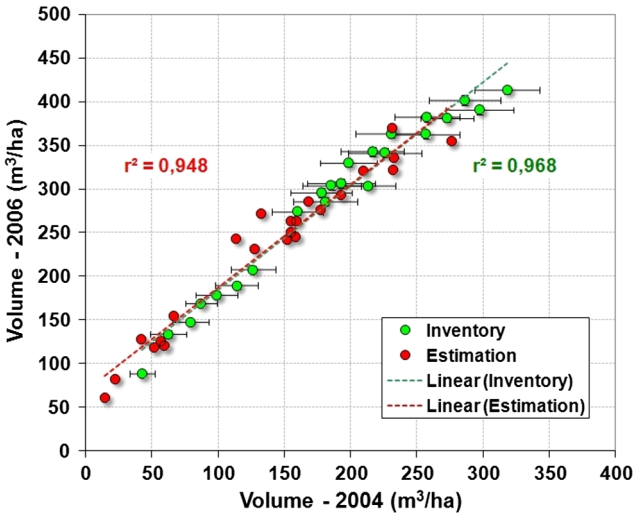

Fig. 12 Tree volume inventoried and estimated.

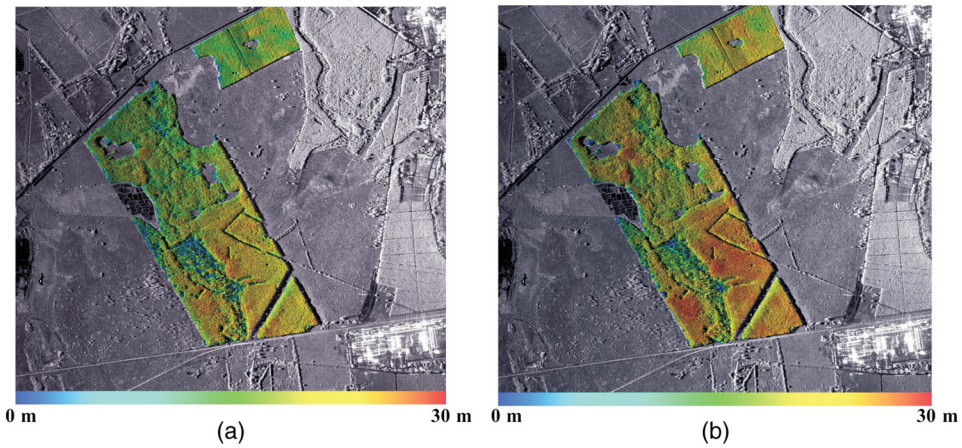

Fig. 13 IHS (I = X-band, H = total height estimation, S = 50%): (a) 2004 estimation and (b) 2006 estimation.

which represented 1.18 m, or 4.84% of prediction error, when compared with higher values of tree heights.

The hypsometric image of Fig. 14(a) was generated using the DBH regression model, and the corresponding SAR data from 2004, obtaining an image whose pixel values correspond to numerical values of the regression, with a spatial resolution of 1.9 m. It can be noticed from Fig. 14(a) that part of the test site has predominance in the DHP values ~10 to ~15 cm. The regions of the image in blue correspond to DHP null values, resulting from the failure of the stand.

The hypsometric image of Fig. 14(b) corresponds to the DBH estimated for 2006, using the regression model generated in 2004, and the SAR data from 2006. Using linear regression with the 2006 inventory data and the DBH model results, MSE of 1.63 cm was obtained, which represented 1.28 cm, or 6.62% of prediction error, when compared with higher values of DBH.

Using the regression model generated in 2004, it was possible to yield an IHS image of the forestry volume, whose results were shown in the hypsometric image of Fig. 15(a). For the obtained color image gradients, it can be noticed that the volume values ranged between 0 and ~400 m^3/ha. The stand failures are represented in blue color, corresponding to low volume values.

The hypsometric image of Fig. 15(b) is an IHS image that corresponded to the volume estimated for 2006, using the regression model generated in 2004, and the SAR data from 2006. The

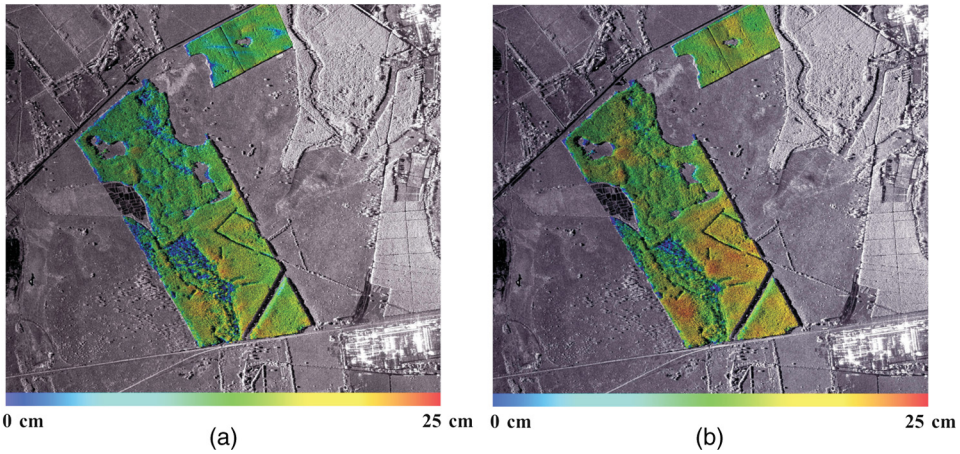

Fig. 14 IHS (I = X-band, H = DBH estimation, S = 50%): (a) 2004 estimation and (b) 2006 estimation.

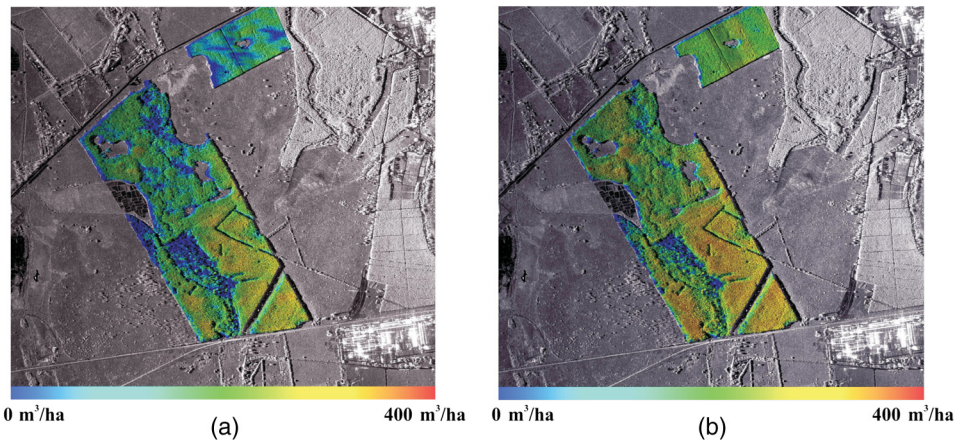

Fig. 15 IHS (I = X-band, H = volume estimation, S = 50%): (a) 2004 estimation and (b) 2006 estimation.

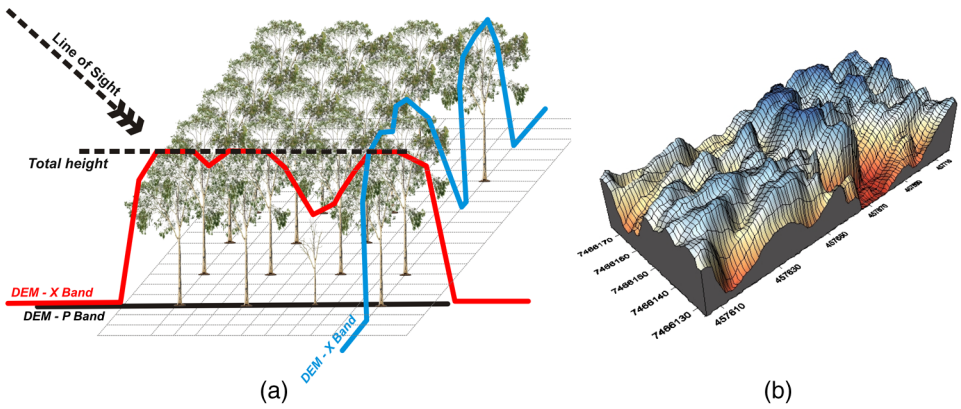

Fig. 16 (a) Gaps and ground truth (red and blue lines: X-band DEM, black line: P-band DEM) and (b) Hint (X-band DEM minus P-band DEM) of the plot showing the gaps effect.

linear regression of the 2006 inventory data and the volume model results, presented a MSE value of 2448.01 m^3/ha, which represented 49.48 m^3/ha, or 11.96% of prediction error if compared with higher values of tree volume.

Although the planting occurred in the same period, the average total height of each transect presented a wide range of values after 4 and 6 years of development, since it is a seminal reforestation and the provision of water and nutrients varies in the area, which hinders the *Eucalyptus* development. Additionally the occurrence of gaps between 2% and 60% inside the plots was verified. So, this characteristic induced intermediate height measurements rather than ground height, disturbing the Hint measurement (X-band DEM minus P-band DEM) that would infer the tree heights, as illustrated in Fig. 16(a) and observed in Fig. 16(b).

As in the regions with trees the Coh in the P-band is high, and in clear areas the P-band coherence is low, the presence of this variable in the total height and DBH models compensated the gap effects, improving the model performance as shown in graphs of Figs. 6 and 7.

When these models were used with the second acquisition data from airborne radar (2006), the estimation errors were a little higher if compared with those of 2004 used as a reference basis. One of the reasons for the slight decrease in performance can be explained by significant differences between Eucalyptus stands of different ages, which result in variations of the morphometric parameters canopy. With the growth of the individual trees tend to have a faster development of the trunk, compared to the development of the crown; i.e., the coverage ratio, salience index and living space index decrease with the growth of trees and the increasing size inside the forest stand. Thus, due to these variations of the percentage of the gaps, consequently the CohPvv and/or Hint contribution did not fit in some cases.

Nevertheless, the errors for DBH and total height models would still be suitable for forest surveying, which considers 10% as a typical inventory error. For volume prediction the error was 1.96% beyond this limit.

6 Conclusions

The use of the biophysical models created in the first imaging campaign, along with field and radar data from the second campaign carried out two years later, were consistent and the results are very promising for updating annual inventories required in Eucalyptus planting management aiming at cellulose production.

For the vegetation volume model, only the X-band interferometric surveying would be necessary for the annual volume estimations, because the model only uses the logHint variable. Therefore, this approach decreases surveying costs, once the generation and processing of new data in P-band would not be necessary, since P-band interferometry demands two passes and X-band interferometry demands only one pass. Another possibility to be evaluated would be the use of X-band interferometry by the satellites TerraSAR/TanDEM or Cosmo SKYMED, in

order to generate the DEM, but it would be necessary to have a P-band or L-band DEM in advance.

We recommend carrying out further research for steep relief, in order to verify its effect on prediction models due to the fact that the area under study in this article is practically flat. As relief variations modify local incidence angle, they can change the target interaction, and in extreme cases cause foreshortening and shadowing effects.

Acknowledgments

The authors acknowledge the help of the 5th Surveying Army Division (Brazilian Army), Nobrecel Celulose and Papel S.A., Diâmetro Biometria & Inventário Florestal, BRADAR Aerolevantamento S.A. (ORBISAT) for their support in this research, and CNPq for a grant received by the second author.

References

1. J. R. Santos et al., "Airborne P-band SAR applied to the above ground biomass studies in the Brazilian tropical rainforest," *Remote Sens. Environ.* **87**, 482–493 (2003).
2. T. Neeff et al., "Tropical forest measurement by interferometric height modeling and P-band backscatter," *Forest Sci.* **51**(6), 585–594 (2005).
3. J. O. Sexton et al., "A comparison of LIDAR, radar, and field measurements of canopy height in pine and hardwood forests of southeastern North America," *For. Ecol. Manage.* **257**, 1136–1147 (2009).
4. F. F. Gama, J. R. dos Santos, and J. C. Mura, "Eucalyptus biomass and volume estimation using interferometric and polarimetric SAR data," *Remote Sens.* **2**, 939–956 (2010).
5. P. C. Bispo et al., "Integration of polarimetric PALSAR attributes and local geomorphometric variables derived from SRTM for forest biomass modeling in central amazonia," *Can. J. Remote Sen.: J. Can. de Teledetection* **40**(1), 26–42 (2014).
6. N. P. Joshi et al., "L-band SAR backscatter related to forest cover, height and aboveground biomass at multiple spatial scales across Denmark," *Remote Sens.* **7**, 4442-4472 (2015).
7. M. Santoro, L. E. B. Eriksson, and J. E. S. Fransson, "Reviewing ALOS PALSAR backscatter observations for stem volume retrieval in swedish forest," *Remote Sens.* **7**, 4290–4317 (2015).
8. Y. Rauste et al., "Radar-based forest biomass estimation," *Int. J. Remote Sens.* **15**, 2797–2808 (1994).
9. K.O. Pope, J.M. Rey-Benayas, and J.F. Paris, "Radar remote sensing of forest and wetland ecosystems in the central American tropics," *Remote Sens. Environ.* **48**, 205–219 (1994).
10. M. Borgeaud and U. Wegmueller, "On the use of ERS SAR interferometry for retrieval of geo- and bio- physical information," in *Proc. of the 'FRINGE 96' Workshop on ERS SAR Interferometry*, Zurich, Switzerland (1996).
11. E. S. Kasischke, J. M. Melack, and M. C. Dobson, "The use of imaging radars for ecological applications—a review," *Remote Sens. Environ.* **59**, 141–156 (1997).
12. S.R. Cloude and E. Pottier, "An entropy based classification scheme for land applications of polarimetric SAR," *IEEE Trans. Geosci. Remote Sens.* **35**, 68–78 (1997).
13. T. Le Toan and N. Floury, "On the retrieval of forest biomass from SAR data," in *Proc. of the 2nd Int. Symp. on Retrieval of Bio- and Geo-physical Parameters from SAR data for Land Applications*, ESTEC, Noordwijk, The Netherlands (1998).
14. D. G. Leckie and K. J. Ranson, "Forestry applications using imaging radar," in *Principles & Applications of Imaging Radar: Manual of Remote Sensing*, R. A. Ryerson, Ed., 3th ed., Vol. **2**, pp. 435–509, John Wiley & Sons, Inc., New York, NY (1998).
15. J. C. Mura et al., "Identification of the tropical forest in Brazilian Amazon based on the MNT difference from P and X bands interferometric data," In *Proc. of IEEE Geoscience and Remote Sensing Symp.*, Sydney, Australia (2001).
16. R. Treuhaft et al., "Tropical-forest biomass estimation at X-Band from the spaceborne TanDEM-X interferometer," *IEEE Geosci. Remote Sens. Lett.* **12**(2), 239–243 (2015).

17. M. Rombach et al., "Newest Technology of mapping by airborne interferometric synthetic aperture radar system," *IEEE Trans. Geosci. Remote Sens.* **7**, 4450–4452 (2003).
18. S. A. Quegan, "Unified algorithm for phase and cross-talk calibration of polarimetric data—Theory and observations," *IEEE Trans. Geosci. Remote Sens.* **32**, 89–99 (1994).
19. M. Zink and R Bamler, "X-SAR radiometric calibration and data quality," *IEEE Trans. Geosci. Remote Sens.* **33**, 840–847 (1995).
20. J. Neter et al., "*Applied Linear Statistical Models*," 4th ed., McGraw-Hill, Boston, MA (1996).

Fábio Furlan Gama graduated in electronic engineering from the Vale do Paraiba University, Sao Jose dos Campos, Brazil, in 1986 and received his MS and PhD degrees in remote sensing from the National Institute for Space Research (INPE), Sao Jose Campos, Brazil, in 1996 and 2007, respectively. He currently works at INPE, as a senior researcher in the Image Processing Department in development and applications of polarimetry and interferometry SAR. His research interests include SAR interferometry, differential SAR interferometry, SAR polarimetry, and applications of SAR surveying for land use/cover.

João Roberto dos Santos received his BSc degree in forestry engineering from the Federal Rural University of Rio de Janeiro, Brazil—UFRRJ in 1974. He received his MSc degree in remote sensing from INPE in 1979 and his PhD in forest science from the Federal University of Paraná—UFPR, 1988. He is a senior researcher in the Remote Sensing Division of INPE, whose current activities are optical and SAR applications for the inventory and monitoring of forest typologies

José Claudio Mura graduated in electrical engineering from the School of Engineering of São Carlos USP, 1978, received his master's degree in electronics and computer engineering from the Technological Institute of Aeronautics, 1985, and his PhD in applied computing from the INPE, 2000. He is a senior researcher at INPE. He has experience in computer science, with emphasis on methodology and technical computing, acting on the following topics: SAR interferometry, SAR polarimetry, and SAR calibration. Currently, he is working in the field of differential interferometric SAR images to estimate surface deformation using orbital radar sensor data